ISBN: 978-3-95450-191-5 doi:10.18429/JACoW-SRF2017-MOPB064

HIGH POWER TEST FOR PLUG-COMPATIBLE STF-TYPE POWER COUPLER FOR ILC

Y. Yamamoto†, E. Kako, T. Matsumoto, S. Michizono, A. Yamamoto, KEK, Tsukuba, Japan
E. Montesinos, C. Julie, CERN, Geneva, Switzerland

Abstract

From the view point of plug-compatibility for the power coupler in the International Linear Collider (ILC), recommended by Linear Collider Collaboration (LCC) in 2013, new STF-type power couplers with 40mm of input port diameter were re-designed, fabricated and successfully high-power-tested. Moreover, from the view point of the cost reduction for the ILC, another type of power couplers with Titanium-Nitride (TiN) coating-free ceramic were also fabricated and high-power-tested by the collaboration between CERN and KEK. In this paper, the detailed results for the both power couplers will be presented.

INTRODUCTION

Following the recommendation by the LCC [1] in 2013, the STF-type power couplers with the plug-compatible design were re-designed and fabricated to meet the specification in the Technical Design Report (TDR) [2] for ILC [3]. Additionally, two cold parts with ceramic window without TiN coating were also fabricated for lower cost study. Therefore, there are two warm and cold parts with the TiN-coated ceramic window, and two cold parts with the coating-free ceramic window, fabricated in 2014, as shown in Table 1. For the test of each type of ceramic, the two warm parts are common, and only cold parts were exchanged each other.

Table 1: Summary of the Plug-compatible STF-type Power Couplers Fabricated in 2014

Coupler	Ceramic vendor	Ceramic colour	Coating
Warm #1, #2	A	White	TiN
Cold #1, #2	A	White	TiN
Cold #3, #4	B	Gray	Free

Table 2 shows the R&D history of the plug-compatible STF-type power coupler. The RF design by HFSS [4] and the mechanical design were simultaneously done. The fabrication for all components of power couplers were completed on November in 2014, delivered to KEK, and the incoming inspection was done there on March in 2015. After the assembly work for the test bench in the clean room, the low power measurement using the network analyser was done, and adjusted the coupling to the waveguide system by changing the insertion length of the inner conductor. The test bench was connected to the high power test area. As for the power coupler with coating-free ceramic, the same thing was done. In the following sections, each item is described in detail.

† yasuchika.yamamoto@kek.jp

RF DESIGN BY SIMULATION

The RF simulation by HFSS was done for the various models as described later. The main changed points from the STF-2 power coupler [5] are the power coupler port of 40 mm, and the wider range of the external Q. In the following sub-sections, the result is described in detail.

Coupling to Cavity

To fix the range of external Q, the coupling to the cavity (the cavity shape is TESLA) was estimated for two models:

- Real end-cell model (for two different diameter)
- Symmetric end-cell model

These two models are shown in the top two figures of Figure 1. For the real end-cell model, the input antenna with two different diameters was tested. The result for external Q is given in the bottom-left figure. From this plot, it is clear that the insertion length ranges within 24 to 36 mm to meet the range of $10^{6\text{-}7}$ for Q_{ext}.

Table 2: R&D History of Plug-compatible STF-type Power Coupler

Date	Content
Nov/2013	Recommendation for plug-compatible design from LCC in LCWS2013 [6]
Feb/2014	Completion of mechanical design
Jun/2014	Completion of RF design by simulation
Nov/2014	Completion of prototype coupler fabrication
Mar/2015	Incoming inspection in KEK
Aug/2015	Assembly work in clean room (Warm #1, #2 + Cold #1, #2)
Dec/2015	Low power test at bench
Jan/2016	High power test at bench
Feb/2016	Dis-assembly, and re-assembly work in clean room (Warm #1, #2 + Cold #3, #4)
Feb/2016	Low power test at bench
Mar/2016	High power test at bench

Full Test Bench Model

After the calculation for the coupling to the cavity, the simulation was done for the full test bench model connected with two power couplers including the bellows to check the RF matching, as shown in the bottom-right figure in Figure 1. It typically took several hours per run to do this simulation. At this time, the waveguide system and the doorknob are the previous type, not optimized for this plug-compatible STF-type power coupler. This might generate the unexpected phenomena with some risks in the both of low and high power tests.

ISBN: 978-3-95450-191-5 doi:10.18429/JACoW-SRF2017-MOPB064

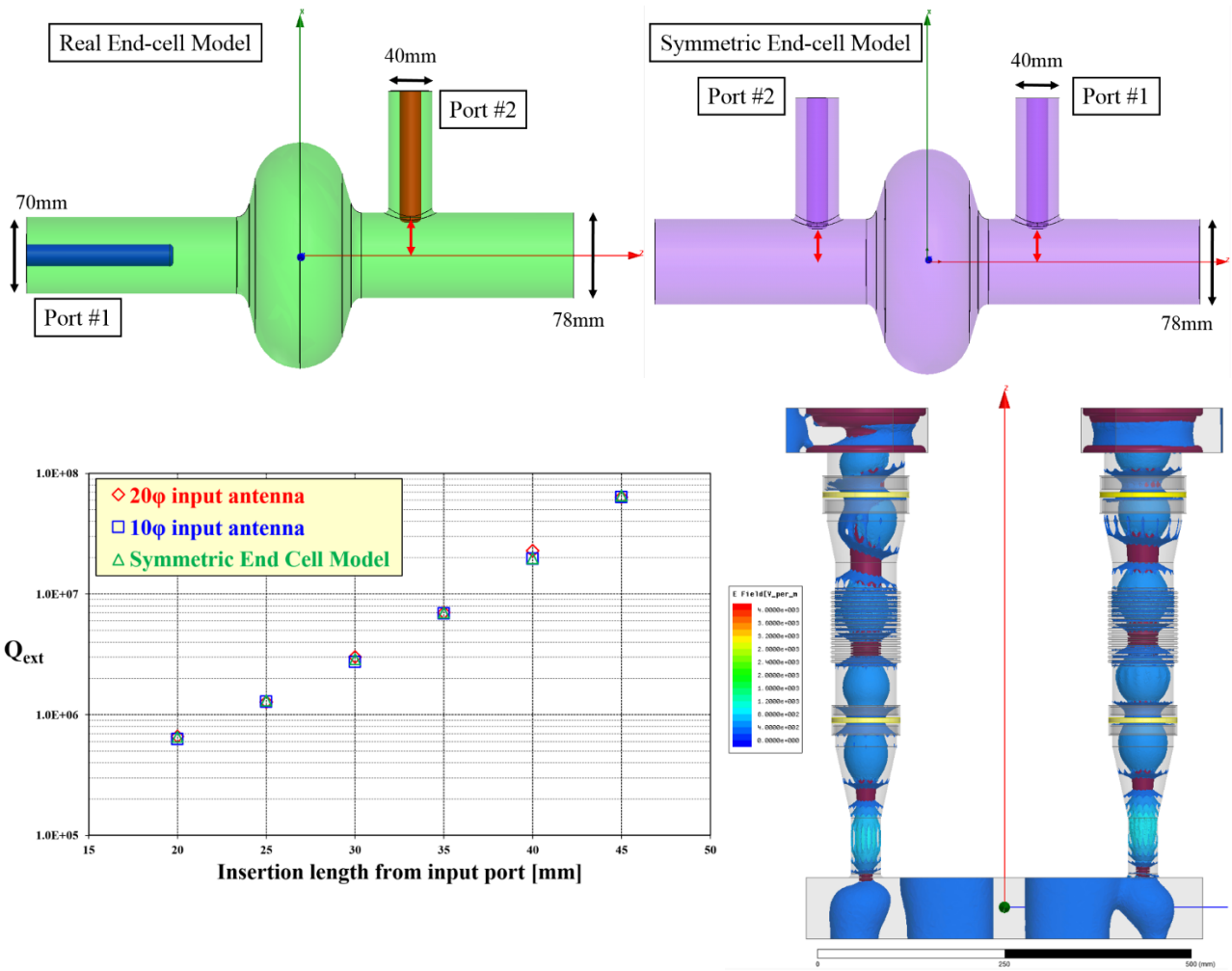

Figure 1: Two models for the calculation of the coupling to the cavity in the top two figures, the correlation plot between Q_{ext} and the insertion length from the port of power coupler (shown as the red arrow in the top two figures) in the bottom-left figure, and the full test bench model with the animation of electric field in the bottom-right figure. For the range of external Q, the necessary specification for ILC is $10^{6\text{-}7}$.

Different Kinds of Ceramic Material

In this R&D, there are two types of ceramics; one is TiN coated ceramic by "Vendor A", and the other is coating-free ceramic by "Vendor B". To investigate the effect by the different type of ceramic, these material parameters were put into the simulation as shown in Table 3. The coating-free ceramic was fabricated under the condition of the lower secondary electron emission coefficient, however, oppositely higher loss tangent, and not optimized yet. Due to the different type of ceramic material, although the RF matching for the test stand was also drastically changed, it enabled the longer bellows attached at the inner conductor of cold part to optimize the matching condition.

Table 3: Comparison of Ceramic Material [7, 8]

Ceramic vendor	Relative permittivity	Dielectric loss tangent	Secondary electron emission
A (TiN)	8.8@10GHz	$6\text{x}10^{-4}$	~2.0
B (free)	10.0@8GHz	$3\text{x}10^{-3}$	3.2

FABRICATION/INCOMING INSPECTION

For the fabrication of the plug-compatible STF-type power coupler, the same procedure was taken as the power coupler installed into the STF-2 cryomodules. The cross-sectional drawing is shown in the top figure in Figure 2. In the bottom-left figure, the connection with the warm and cold parts is shown. The copper plating by pyrophosphate was used for the both surfaces of the outer and inner conductors, and the condition is shown in Table 4.

At the incoming inspection after the delivery to KEK, many blisters on the head of the inner conductor in Cold #1 were observed as shown in the bottom-right figure in Figure 2. The cause for this phenomena is described in detail in this conference [9]. Although the unexpected phenomena might occur at the head in the high power test, it was decided to proceed to the assembly work in the clean room due to the time schedule. As described later, consequently, the unexpected phenomena for Cold #1 did not occur during the high power test.

ISBN: 978-3-95450-191-5 doi:10.18429/JACoW-SRF2017-MOPB064

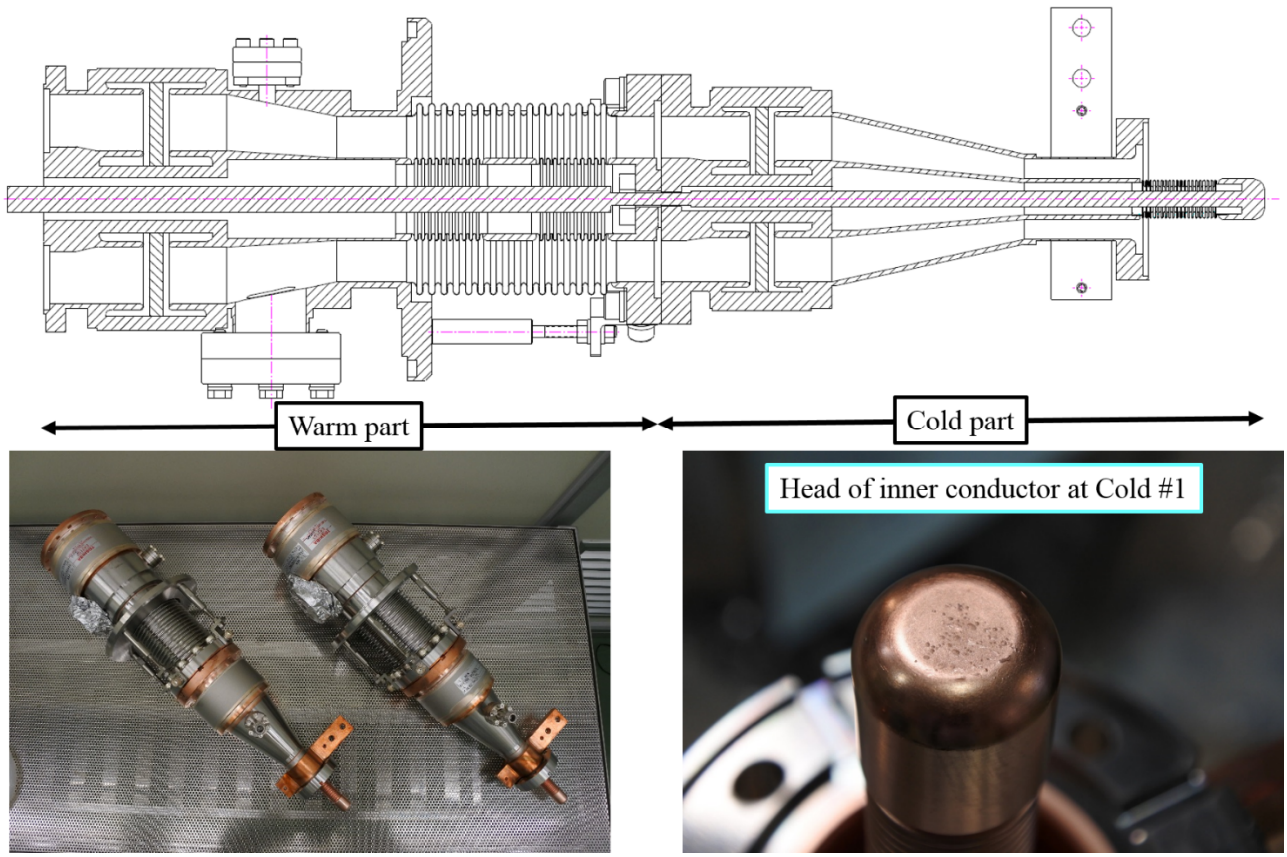

Figure 2: Cross-sectional drawing of the plug-compatible STF-type power coupler (top), connection of the warm and cold part (bottom-left), and many blisters generated on the head of the inner conductor of Cold #1 (bottom-right).

Table 4: Summary of Copper Plating Condition

Warm inner	Warm outer	Cold inner	Cold outer
25μm Gold strike	25μm Nickel strike	25μm Gold strike	10μm Gold strike

ASSEMBLY WORK IN CLEAN ROOM

After the incoming inspection, the assembly work for the test bench was done in the clean room of Class 10 (ISO 6) in STF. Only the cold parts were rinsed by the ultrapure-water for a few minutes, and the warm parts were cleaned up by the ion gun, not rinsed. The vacuum parts were rinsed by the ultrasonic (1100W, 40kHz, 63liter, 25℃ of water temperature) and the detergent (FM-20). All components were dried in the Class 10 area during one night. In the next day, the assembly work was done there. As for the vacuum sealing, the aluminium hexagonal sealing was used for the connection between the cold part and the waveguide system, the two types of helico-flex for the connection of the inner/outer conductor between the warm and the cold part, and the indium wire for the connection of the waveguide system.

After the assembly work, the pumping was done for the leak check. In STF, usually, the leak check is done at the vacuum level below 10^{-3} Pa, and the leak rate of 10^{-10} Pa·m^3/sec. The baking is done at 100℃ for the power coupler, and 90℃ for the waveguide system for over 48hours. The cause for the lower temperature baking is the use of the indium wire. After the baking, the both vacuum level becomes around 10^{-6} Pa at the room temperature. Figure 3 shows the status of the assembly work, the pumping/leak check, and the baking in STF. The next step is the low power test by the network analyser.

LOW POWER TEST/ADJUSTMENT

After the baking, the low power test was done using the network analyser (E5061B). The purpose is the adjustment of the coupling to the waveguide system by changing the insertion length of the inner conductor. The result is shown in Figure 4, and S_{11} at minimum was below -45dB. As expected before, the result was different between the TiN-coated ceramic and the coating-free ceramic. Fortunately, S_{11} for the both types were adjusted below -30dB at minimum. After the adjustment, the test bench was connected to the high power test area.

HIGH POWER TEST

The 5MW klystron was used for the high power test. The operational condition is shown in Table 5. Figure 6 (top) shows the high power test stand in STF. The monitoring signals are the both vacuum of the warm and cold parts, the electron emission detected by the peak-hold module [10], the arc detector output, the forward/backward power at the both directional couplers in the upstream and downstream of the test stand, and the temperature at each position.

ISBN: 978-3-95450-191-5 doi:10.18429/JACoW-SRF2017-MOPB064

Figure 3: Status of the assembly work in the clean room, the baking, and the low power test by the network analyser. From left to right in the top figures: the ultrapure water rinsing, cleaning by the ion gun, and jointing between the warm and cold parts. From left to right in the bottom figures: the pumping and the leak check, the baking, and the low power test.

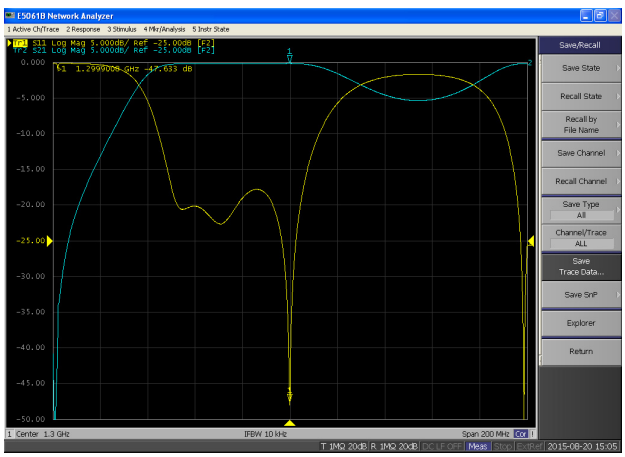

Figure 4: S parameters (Yellow: S_{11}, Blue: S_{21}) after the adjustment for the test bench of the plug-compatible STF-type power coupler.

The technical interlock (TIL) for the vacuum level is 2 x 10^{-4} Pa, the other TILs are the forward/backward power limit, and the arc output limit.

The RF conditioning started from 10μsec/5Hz, and finished at 1500μsec/5Hz using the auto-conditioning module and the vacuum distributor module delivered from CERN [11]. Above 1500μsec, the heating effect at the inner conductor of the cold part is not negligible due to the higher RF duty. Then, the RF conditioning is sometime stopped around 700 kW. The outside of the power coupler is cooled by fans. Figure 5 shows the status of the forward/backward power and the both vacuum levels (left), the luminescence observed in the cold parts (center), and correlation plots between the cold vacuum level and the electron emission (Electron #1: upstream, Electron #2: downstream) for the forward power (right). The electron emission is evaluated by the peak height (right-top) and the total charge (right-bottom) in each pulse.

The total conditioning time was about 92hours for the plug-compatible STF-type power coupler with the TiN-coated ceramic. No unexpected event was observed in the cold #1 with many blisters. Consequently, the plug-compatible STF-type power coupler was successful. On the other hand, as for the coating-free ceramic, the conditioning time below 500μsec was shorter, because the warm parts are common as shown in the bottom figure in Figure 6. However, during the RF conditioning in 1500μsec, unusual heating was observed at the tapered pipe of the cold part around 480 kW, and also the cold windows. Simultaneously, the electron emission suddenly increased up to the maximum level (10 V). As the result of various coupler combination tests, it was clear that the only power couplers with the coating-free ceramic had unusual heating around the tapered pipe of cold part. Presumably, this cause is due to the coating-free ceramic, which has the higher secondary electron emission coefficient. At present, the electron tracking simulation by CST Particle Studio is under progress.

Table 5: Operational Condition of High Power Test

Pulse width [μsec]	Repetition rate [Hz]	Max. power [kW]
10	5	1200
30	5	1200
100	5	1200
500	5	1200
1500	5	800
1650	5	~700

ISBN: 978-3-95450-191-5 doi:10.18429/JACoW-SRF2017-MOPB064

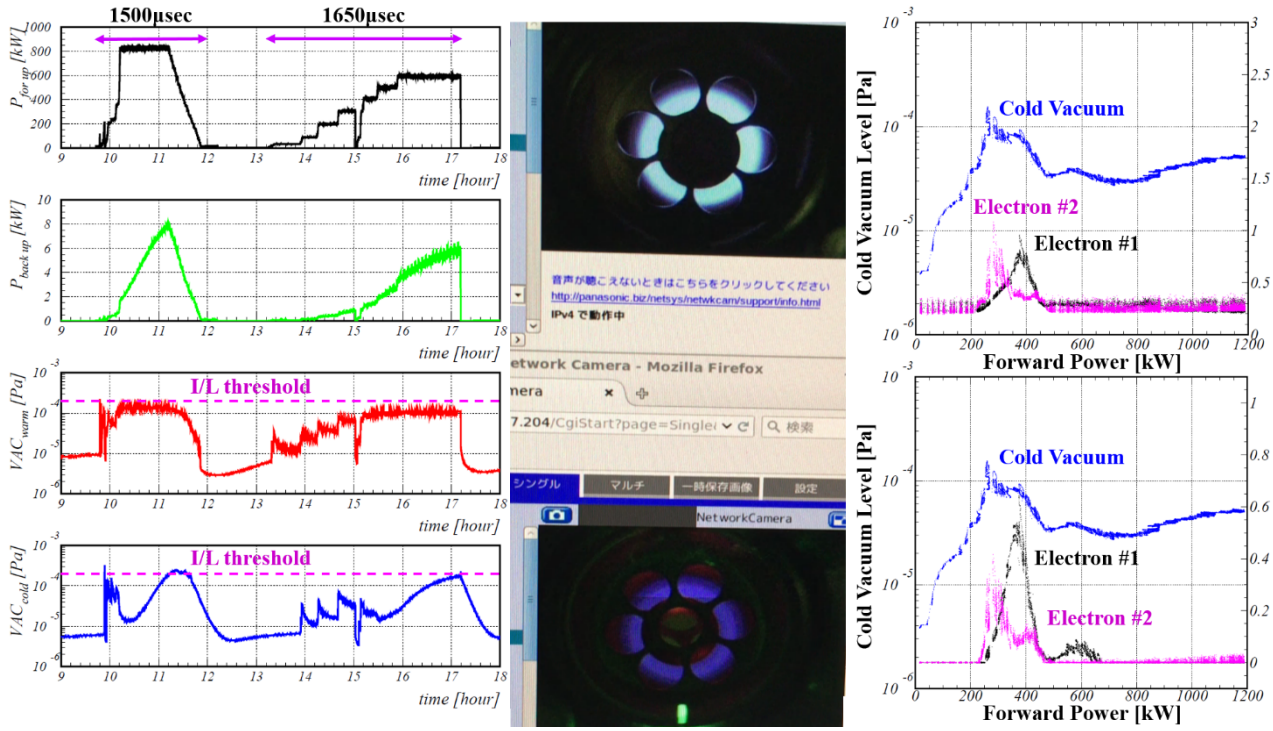

Figure 5: Left figure shows the trend graph for the forward/backward power, and the both vacuum of the cold and warm part which technical interlock threshold is 2 x 10^{-4} Pa shown as the purple dotted line. Center figure shows the luminescence in the both cold parts during the high power test. Right figure shows the correlation plots between the cold vacuum level and the electron emission (Electron #1: upstream, Electron #2: downstream) for the forward power.

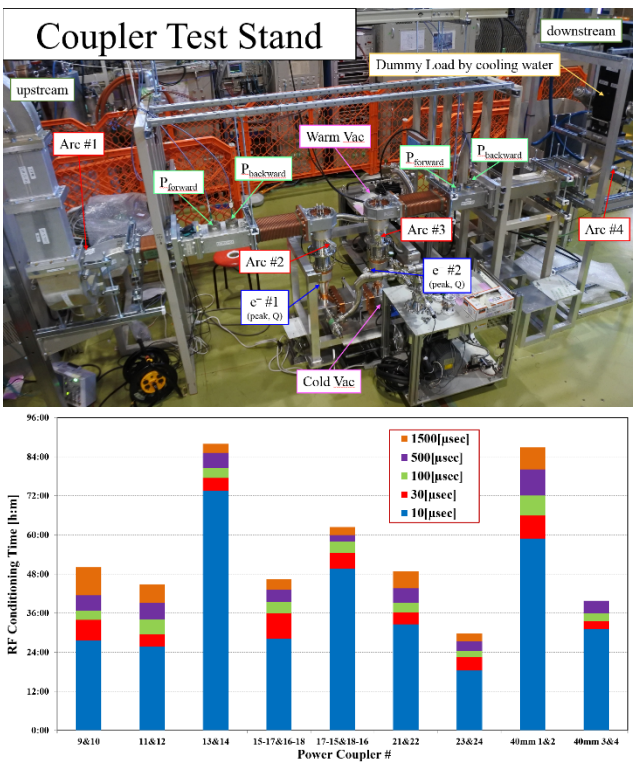

Figure 6: High power test stand (top), and summary of RF conditioning time for every power coupler in STF (bottom). "40mm 1&2" is the power coupler with the TiN-coated ceramic, and "40mm 3&4" is the coating-free. #9-#10 were used for the capture cryomodule, and #11-#24 for the STF-2 cryomodules.

CONCLUSION

After the recommendation by LCC in 2013, the plug-compatible STF-type power coupler was designed, fabricated, inspected, assembled, and low/high-power-tested. The result for the TiN-coated ceramic was successful, and however, more R&D is necessary for the coating-free ceramic. Recently, new R&D programs for the STF-type power coupler started, and the first result is presented in this conference [9].

ACKNOWLEDGEMENT

Special thanks are given to T. Yanagimachi, S. Imada, M. Asano (NAT), and R. Ueki (moved from NAT to KEK) for the operation in the RF conditioning; N. Hanaka, K. Ishimoto, and N. Numata (NAT) for the LLRF/HLRF control system; T. Okada (K-VAC) for the assembly work of the test bench in the clean room; A. Hayakawa (KIS) for the maintenance of control and monitoring system for the operation of RF conditioning.

REFERENCES

[1] Linear Collier Collaboration, https://www.linearcollider.org/

[2] ILC Technical Design Report (2013). https://www.linearcollider.org/ILC/Publications/Technical-Design-Report.

[3] International Linear Collier, https://www.linearcollider.org/ILC

[4] High Frequency Structural Simulator, http://www.ansys.com/products/electronics/ANSYS-HFSS

ISBN: 978-3-95450-191-5 doi:10.18429/JACoW-SRF2017-MOPB064

[5] E. Kako *et al.*, "Advances and Performance of Input Couplers at KEK", Proceedings of SRF2009, pp. 485-490, Berlin, Germany.

[6] LCWS 2013, http://www.icepp.s.u-tokyo.ac.jp/lcws13/

[7] https://www.ngkntk.co.jp/english/product/list/property.html

[8] K. Iwamoto *et al.*, "Preliminary Study of Low SEE Coefficient Alumina for Coupler Window", TTC Meeting 2014, KEK, Japan.

[9] Y. Yamamoto *et al.*, "Fundamental Studies for the STF-type Power Coupler for ILC", MOPB063, SRF2017, Lanzhou, China.

[10] Y. Yamamoto *et al.*, "Development of Peak-hold Module for Electron Emission in STF-type Power Coupler for the ILC", Proceedings of IPAC2017, pp. 1034-1036, Copenhagen, Denmark.

[11] Y. Yamamoto *et al.*, "STF-2 Cryomodule Performance and New Input Coupler R&D for ILC", PoS(ICHEP2016)066, ICHEP2016, Chicago, U.S.